Wind Tunnel Experiments Relating to Supersonic and Hypersonic Boundary-Layer Transition

J. M. KENDALL*

Jet Propulsion Laboratory, Pasadena, Calif.

Hot-wire anemometry is used to study the origin and growth of "natural" fluctuations in zero pressure-gradient boundary layers for several Mach numbers between 1.6 and 8.5. The importance to transition of certain physical mechanisms is examined through comparison of the fluctuation growth with the sound-forcing and stability theories of Mack. Flow fluctuations of substantial amplitude were observed within the laminar layer ahead of stations where instability amplification is expected to be important. These fluctuations were found to be cross-correlated with the sound field for the higher supersonic speeds, but not for the lower ones. The fluctuation growth rates in the unstable Reynolds number range ahead of the nonlinearity region were in reasonably close agreement with the theory for Mach 4.5; the agreement for Mach 2.2 and 8.5 was qualitative. The second mode of instability was predominant at Mach 8.5.

Nomenclature

$A(f)$ or A = fluctuation amplitude within a frequency band centered at f
c_p = wave phase speed
$e_f{}^2$ or e^2 = hot wire signal energy within a frequency band centered at f
f = circular frequency
F = dimensionless frequency, $2\pi f/u_1 Re$
l = cone length
M = mach number
r_{12} = cross-correlation coefficient
R = $Re_x{}^{1/2}$
Re = unit Reynolds number
Re_x = Reynolds number based on length
T_w = wall temperature
T_{aw} = adiabatic wall temperature
u = flow velocity
x = length, measured from plate leading edge or cone tip
y = dimension normal to surface
α_i = dimensionless amplification rate
δ = boundary-layer thickness
θ_c = cone half angle
τ = time delay of signal e_1
ψ = wave obliqueness angle, measured from cross-flow direction

Subscripts

∞ = value in tunnel freestream
1 = value at boundary-layer edge, equal to ∞ condition for flat plate case
o = value at neutral stability point

I. Introduction

THE premise of the experiments described here is that an understanding of transition can best be gained by studying the onset and growth of flow unsteadiness in the region of a boundary layer ahead of transition, rather than by recording its movement in response to a change of parameter. In particular, the goal has been to identify and measure the various physical mechanisms relating to: a) the source of flow unsteadiness, such as freestream turbulence, sound waves, or vibrations; b) the means by which such unsteadiness drives the laminar boundary layer of interest; c) the chain of amplification mechanisms by which small disturbances assume the proportions and characteristics of turbulence.

Morkovin[1] has described this as the "microscopic" approach in his evaluation of the high-speed transition problem. This most-illuminating document is required reading for all who wonder why a research program is yet needed after 25 years of transition testing.

The experiments have of necessity been carried out in a wind tunnel, there being no possibility at present of making sufficiently detailed measurements in any other type of facility. As is now well known, the wind tunnel environment is noisy. Laufer[2] pointed out 15 years ago that the freestream of a conventional supersonic tunnel suffers a high sound intensity because of radiation from the turbulent boundary layers on the tunnel walls, and that this sound can constitute an important source of disturbance energy to the laminar layer on a test model. He went on to study the sound field in some detail,[3,4] indicating its dependence upon the wall friction coefficient and determining the intensity and source convection speed as a function of Mach number, M_∞. Together with certain measurements made by others[5,6] it appears that the rms pressure fluctuation in ratio to the static pressure, p'/p_∞, can be represented approximately by a constant times $M_\infty{}^2 Re^{-0.3}$ for $1.6 \leqq M_\infty \leqq 8$, where Re is the unit Reynolds number. The constant is expected to depend upon the tunnel size and geometry. Some measurements of the sound spectra have also been reported.[4-6] By way of illustration, p'/p_∞ is of the order of 2% at $M_\infty = 5$, and the spectrum shows energy to well over 100 kHz.

There is little doubt concerning the importance of this sound. Pate and Scheuler[7] devised a correlation parameter which brought transition data from several tunnels of widely different size and operated at variable unit Reynolds number into coincidence when plotted against the tunnel wall friction coefficient. Moreover, experiments at $M_\infty = 4.5$ in the JPL supersonic tunnel[8] showed that by operating the tunnel at a low pressure to avoid wall turbulence, transition did not occur on a test plate at $Re_x = 3.3 \times 10^6$. According to the unit Reynolds number variation commonly observed, it would have occurred at less than 1×10^6, had the layers been turbulent.

Laufer[9] also considered freestream vorticity and temperature fluctuations as factors affecting transition. He showed that the supply section fluctuation level in the JPL 20-in. tunnel could be reduced to less than 1% by means of damping screens. Transition on a test model was determined for three Mach

Presented as Paper 74-133 at the AIAA 12th Aerospace Sciences Meeting, Washington, D.C., January 30–February 1, 1974; submitted April 3, 1974; revision received October 4, 1974. This paper presents the results of one phase of research carried out at the Jet Propulsion Laboratory, California Institute of Technology, under NASA Contract NAS7-100.

Index category: Boundary-Layer Stability and Transition.

* Group Supervisor, Physics Section. Member AIAA.

numbers under the condition of this low turbulence level, and also with the level intentionally increased by an order of magnitude. Transition was affected only for $M_\infty \gtrsim 2.5$, and only modestly even then. Thus, sound seems to be the most important source of disturbances under normal supersonic test conditions.

Our knowledge of supersonic amplification mechanisms comes mostly from the theoretical work of Mack.[10-12] Some experiments on amplification have been carried out,[8,13,14] but these have been principally aimed toward verification of the theory. In addition, the experiments of Potter and Whitfield[15] and of Staylor and Morrisette,[16] although not directed toward identification of physical mechanisms, give a general indication of some of the results to be presented here. Demetriades[17] has recently presented hypersonic results which both support and extend those to be described here.

The major portion of Mack's work pertains to the stability theory for compressible, zero pressure-gradient flows. The theory yields a prediction of the growth or damping of free oscillations of the layer without regard for the absolute amplitude, except that nonlinearity is excluded. Thus the theory gives growth ratios over a specified length of the boundary layer, but it cannot indicate where nonlinearity and transition will occur. Supplementary information or assumptions are needed for transition prediction. Reshotko[18] has used dimensional considerations to indicate where nonlinearity and transition will occur. Sup-instability constitutes the dominant mechanism of amplification.

There are three general results of the theory of particular importance to the transition problem. First, the theory shows that there can be more than one mode of instability contributing to the fluctuation growth, at least for $M_\infty \gtrsim 4$. The lowest frequency or first mode is similar to the Tollmien-Schlichting instability of incompressible flows, while the second and higher modes are unique to compressible flows. Second, the first-mode waves are most unstable for obliqueness angles, ψ, of about 40°–60°, while second-mode waves are most unstable when in the two-dimensional configuration, $\psi = 0°$. Third, the growth or damping of waves is strongly frequency-dependent, especially for the higher modes. Experimental confirmation of these three general results has been more successful[8] at $M_\infty = 4.5$, than at lower and higher speeds.[13,14]

It was determined early in the present program[19] that a mechanism other than that of instability was operative at $M_\infty = 4.5$. Fluctuations of all frequencies were observed to grow monotonically larger in the region of a boundary layer extending from the flat plate leading edge to the predicted location of instability, i.e., in a region where no growth was expected. A similar result can be inferred from the aforementioned experiments.[15,16] In an attempt to account for these observations, Mack extended his theory to include the response of a layer to incoming sound waves.[11] This forcing theory gives realistic trends; fluctuations of all frequencies are predicted to grow rapidly larger with increasing distance behind the leading edge, and to reach a broad peak at some Reynolds number in the vicinity of that for which instability amplification starts. In general, the response shows a weaker dependence on ψ and on frequency than does the stability theory.

A significant consequence of the forcing theory is that it is then possible in principle to set the absolute value of the fluctuation amplitude for the stability theory, and according to which transition trends may be considered. Provided that the sound characteristics, including frequency and obliqueness distributions, can be measured in a particular environment, then the forcing theory predicts the state of the boundary layer near the beginning of the instability region. The manner in which a forced wave turns into a free one has yet to be determined, however.

With the foregoing as background, the present experiments attempt to examine certain characteristics of the tunnel sound, the efficiency of conversion to boundary-layer fluctuation, the assignment of fluctuation growth to forcing or to a particular mode of instability, and to assessing the limits of linear development. The goal is to gain an understanding of the transition problem in general, rather than to understand transition in a tunnel in particular; however, this is not an easy task, as is already well known.

II. Equipment and Methods

The supersonic testing was performed in the JPL 20-in. continuous flow tunnel. The test section is 45 cm wide, 50 cm high, and the length to the throat varies from about 150 cm to 250 cm as M_∞ increases from 1.6 to 5.6. All flat-plate experiments were carried out in this tunnel on a steel plate 35 cm long which spanned the tunnel width. The 10°-beveled leading edge was as sharp and uniform as practical, and was inspected for defects at frequent intervals.

The hypersonic testing was performed in the JPL 21-in. continuous flow tunnel at $M_\infty = 8.5$, except for a brief test at $M_\infty = 5.0$. The test section is 50 cm wide, 54 cm high, and the nozzle length is 400 cm. For $M_\infty = 8.5$, the supply pressure range was 800 to 2500 cm Hg, and the supply temperature was 645 K. A 4° half-angle cone 96 cm long was tested, giving an edge Mach number $M_1 = 7.7$, $Re_1 = 3.4 \times 10^4$ cm^{-1} to 10.7×10^4 cm^{-1}, and an edge velocity of 1.10×10^5 cm sec^{-1}.

The cone was constructed in two sections consisting of a solid copper demountable tip 14.0 cm long, and a main section containing coolant flow passages. The coolant, nitrogen gas derived from LN_2, was manually controlled. Four thermocouples were incorporated into the cone: one at the base of the tip at dimensionless length $x/l = 0.137$, and the others at 0.415, 0.657, and 0.922. The temperatures recorded at these stations during most of the measurements, expressed in ratio to adiabatic, were $T_w/T_{aw} = 0.56$, 0.65, 0.50, and 0.57. A concern over the streamwise nonuniformity was partly alleviated by the finding that the amplification rates to be presented were not affected by a change of the average temperature by an amount equal to the variance.

All measurements were made with the cone aligned to be precisely parallel with the tunnel axial centerline. Although the flow uniformity of this tunnel is excellent (Mach number variation less than 0.04 m^{-1} along the axis), there could have been asymmetries which influenced the cone boundary-layer thickness or profile shape, which in turn would affect the accuracy of the results. This possibility deserves future attention.

All measurements of the flow reported here were made by means of constant-current hot-wire anemometry. The hot-wire length was 0.03 cm. For $M_\infty \leqq 5.6$, the diameter was 0.00012 cm, and for $M_\infty = 8.5$ it was 0.00025 cm. The frequency-compensation circuit noise limited the frequency range to about 50 kHz in the freestream, and to about 100–200 kHz in the boundary layer depending on the flow conditions. For the flat plate measurements, the probe was supported on an x-y-z traverse, and the lateral uniformity of the fluctuation development was always checked as a matter of course. The cone measurements were carried out using x and y components of motion only. However, the cone was supported on a roll-support mechanism, and the uniformity of development as the cone roll varied was checked.

The vertical position of the probe, y, could either be set at any particular height, or it could be controlled by a servomechanism such that the probe followed a constant value of y/δ during an axial or lateral sweep. δ is the boundary-layer thickness. This was accomplished through a sensing of the overheat of the wire for a fixed heating current. A second servomechanism was used to control the wire current such as to maintain constant overheat during vertical traverses through the layer, thereby keeping the wire sensitivity more nearly constant. The use of either servo precluded the simultaneous use of the other.

Profiles of the fluctuation energy $e_f{}^2(y/\delta)$ were obtained by traversing the hot-wire at constant overheat through the boundary layer at various values of x for particular settings of the wave analyzer frequency, f. For $M_\infty \geqq 3.0$, the profile shapes were relatively independent of f and of x, except near

the onset of transition. $M_\infty = 3.0$ is an unusual case in that the profiles showed two nearly equal amplitude peaks. This will be mentioned further in discussing the cross-correlation results. For all higher speeds, only a single peak was observed. For $M_\infty = 1.6$ and 2.2, the profiles showed a single peak for the lower frequencies which contain most of the energy, and double (but not necessarily equal) peaks for the higher frequencies. The streamwise development of the profiles was somewhat nonsimilar for all frequencies, as discussed by Laufer and Vrebalovich.[13]

A complete description of the flow would require measurement of all fluctuation characteristics such as rms amplitude, spectra, propagation speed, etc., as functions of both y/δ and x. As a matter of practicality, the present measurements were made by placing the hot wire at the vertical location of the wideband energy peak, and taking the results obtained there to characterize the fluctuations prevailing at that particular x station. A quantity $A(f)$ was obtained by taking the square root of the energy spectrum (after subtraction of the electronic noise) measured at any such vertical location, and a quantity $A_\infty(f)$ was determined similarly by placing the hot wire in the freestream. The dependence on f is omitted in the notation used subsequently; A/A_∞ is understood to pertain to the ratio prevailing at the frequency of the independent variable.

The quantities A and A_∞ can be interpreted as being nearly proportional to the mass-flow fluctuation amplitudes. The computed hot-wire sensitivities to mass flow and temperature fluctuations are approximately the same in the layer as they are in the stream for a particular overheat. Mode diagram measurements show that the ratio of the temperature to mass-flow fluctuation is higher in the stream than in the boundary layer. Because of this, the ratio A/A_∞ was dependent on the overheat setting. However, for the value of the overheat used, mostly 30%, the relative temperature response was largely suppressed.

Some measurements of the correlation coefficient $r_{12} = \langle e_1 e_2 \rangle / (e_1^2 e_2^2)^{1/2}$ where e_1 and e_2 are the fluctuation signals of two hot-wire probes, and $\langle\ \rangle$ denotes the time average, were obtained. For all such measurements reported here a delay line and an analog multiplier module were used.

Dimensionless spatial amplification rates α_i were determined from the growth rates of the fluctuations of various frequencies. For the hypersonic test, x-y recorder traces of the fluctuation energy e_f^2 vs x were obtained for 24 frequencies between 5 kHz and 136 kHz. For the supersonic results, faired curves of A/A_∞ vs R for various frequencies were prepared. The amplification rates were determined from

$$\alpha_i = (-1/4e_f^2)(de_f^2/dR) = (-1/2A)(dA/dR)$$

where $R = (Re_x)^{1/2}$ is based on the length along the plate or cone. The frequencies were made dimensionless according to $F = 2\pi f/u_1 Re$, where u_1 is the velocity at the edge of the layer and Re is the unit Reynolds number there.

III. Results

A. Freestream Spectra

Figure 1 presents the normalized spectra measured in the tunnel freestream for several Mach numbers up to 5.6, and for the flow outside the laminar boundary-layer edge on the 4° cone at $M_\infty = 8.5$, $M_1 = 7.7$. The frequency for this latter case was made dimensionless using the freestream conditions. All ordinates have been normalized such that the areas under the curves are equal. Note that Re is not the same for all values of M_∞, and that this has the effect of expanding or contracting the data values along the frequency and energy coordinates in opposition.

In particular, the $M_\infty = 4.5$ data were obtained at a higher value of Re than for any other M_∞. This case was selected for presentation in preference to others that are available at lower values of Re for a definite reason. The spectra measured at this Mach number for $3.0 \gtrsim Re \times 10^{-4}$ cm $\gtrsim 5.0$ show an unusually high energy content in the low-frequency region $f \gtrsim 4$ kHz.

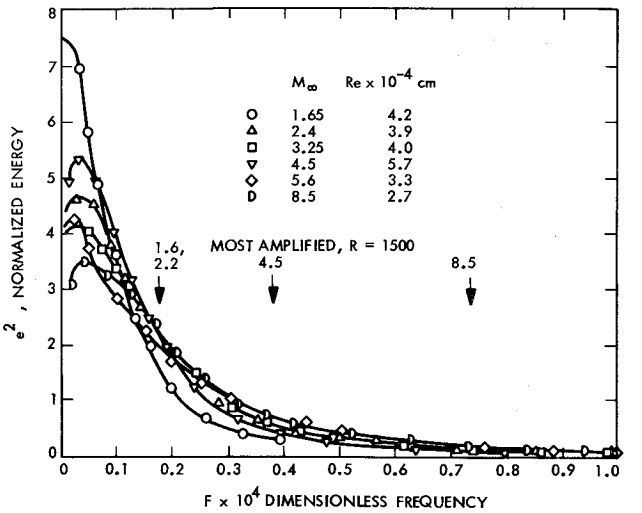

Fig. 1 Freestream spectra, $M_\infty = 1.6$ to 8.5.

This observation was made repeatedly throughout the test program, and was reinforced by the finding that the signals of two hot-wire probes separated laterally by 5.6 cm showed strongly increased correlation in this Re range. This behavior might have been caused by unsteady flow separation in the tunnel contraction section, but this is pure speculation.

A systematic set of measurements of the rms fluctuation amplitude has not been carried out here. Those data that have been obtained at $M_\infty = 1.6$, 2.2, and 4.5 are consistent with Laufer's results.[3,4] His results can be used to provide the Mach number scaling of the spectra for $M_\infty < 5$. Extrapolation or use of the data of Stainback, Fischer, and Wagner[5] may suffice for higher speeds.

An indication of the frequencies expected to be of particular importance to the transition process at various speeds is included in the figure. The arrows denote the frequency of the waves which are most amplified at $R = 1500$ according to stability calculations. The $M_\infty = 8.5$ result is for second-mode waves, while all others are for first-mode waves.

Figure 2 presents the normalized freestream spectra for $M_\infty = 2.4$ at several values of Re. The dimensional data from which these spectra were determined show considerably less variation with Re than that seen here, with the high-frequency energy increasing only slowly with increase of Re. Also shown in the figure is the theoretical quadratic response, i.e., the square of the amplitude response for $R = 1500$, $\psi = 60°$, from Mack's calculations. The ordinate of this curve is drawn with arbitrary scale; the square of the peak response is 240 in actuality. The curve is intended to indicate the range of frequencies of

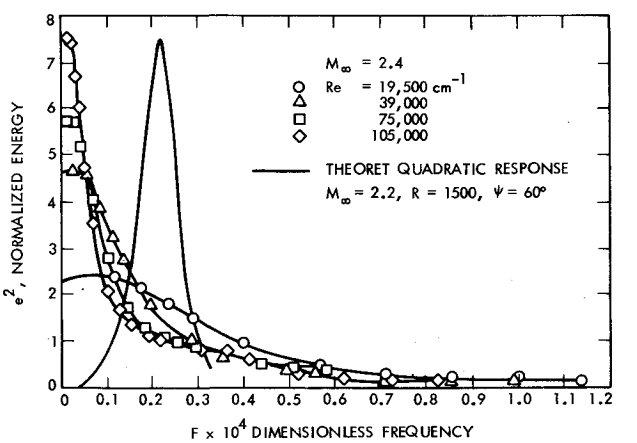

Fig. 2 Freestream spectra, $M_\infty = 2.4$.

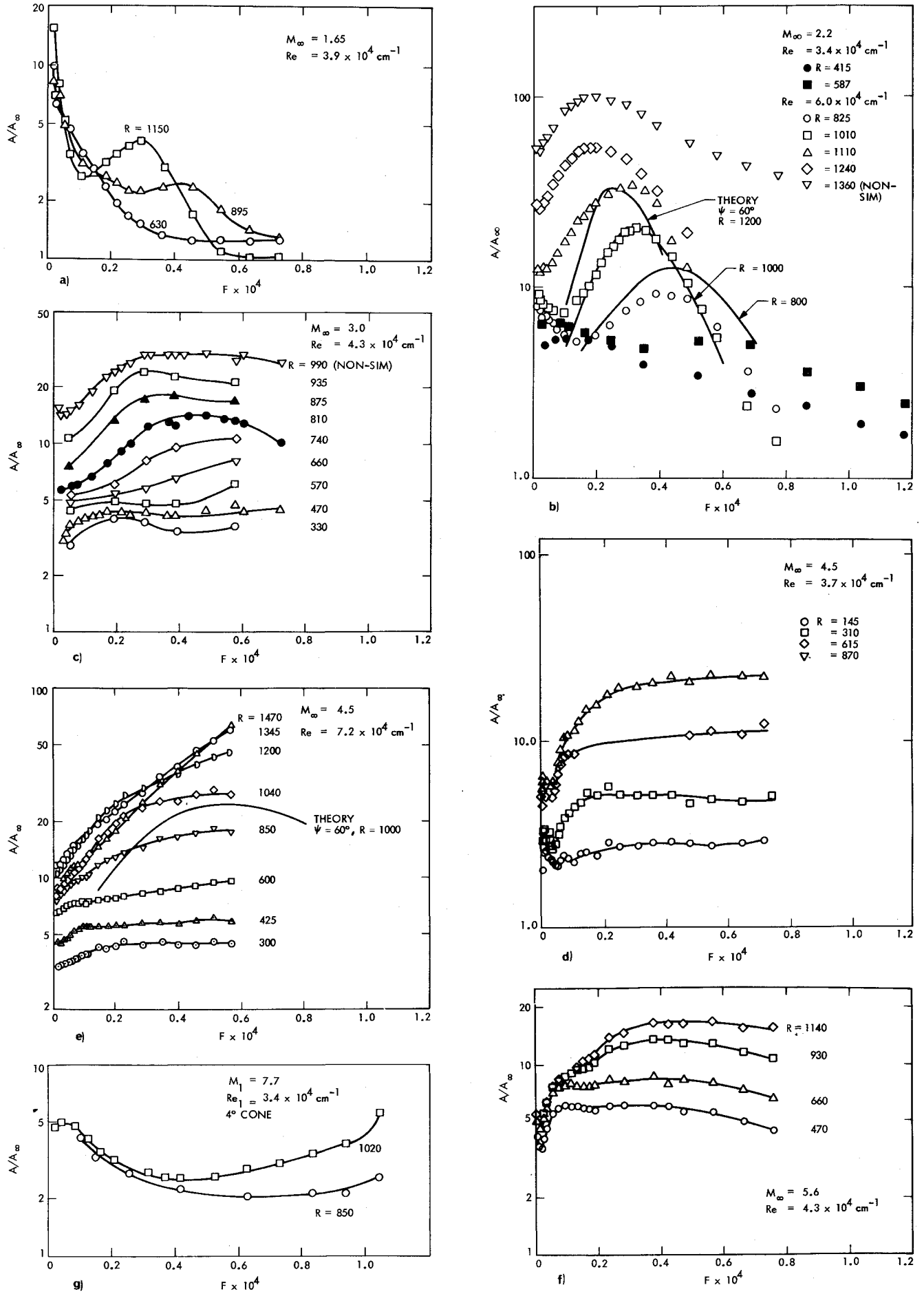

Fig. 3 Boundary-layer frequency response: a) $M_\infty = 1.6$, b) $M_\infty = 2.2$, c) $M_\infty = 3.0$, d) $M_\infty = 4.5$, e) $M_\infty = 4.5$, f) $M_\infty = 5.6$, and g) $M_\infty = 8.5$.

importance according to the stability theory. The slight difference of M_∞, 2.2 to 2.4, is not believed to be important.

The variation of the fluctuation amplitude with Re, to be used in scaling these spectra, has not been measured. The empirical relation in which the amplitude varies as $Re^{-0.3}$ and the energy varies as $Re^{-0.6}$ may suffice for some purposes.

B. Frequency Response Results

Figures 3a–3g present the response curves obtained at several values of M_∞ by comparing the hot-wire signal in the flat-plate boundary layer to that in the freestream ahead of the plate, except for $M_\infty = 8.5$ where the cone layer fluctuations are compared to those outside the layer at about 4δ, $x/l = 0.55$.

The abscissa of the figure is the dimensionless frequency. The amplitudes A and A_∞ have been identified with a fluctuation of the mass-flow. However, the hot-wire response when operated at a high, constant overheat is proportional to the average local mass flow, which is lower in the boundary layer than elsewhere. Thus it follows that the values of A/A_∞ lie below the ratio of the absolute mass-flow fluctuations.

It should also be considered that A was measured at the same vertical location in the layer for all frequencies, and that a larger result could have been attained in some cases by searching out the peak pertaining to a particular frequency. The largest such increase observed in a few detailed studies, about 50%, occurred for $M_\infty = 2.2$, $R = 1300$, i.e., near transition. According to the foregoing, the response curves are necessarily somewhat qualitative.

The most apparent features of the response curves are the over-all levels, the growth rates, and the spectral distributions. The cases $M_\infty = 1.6$ and 2.2 are distinctive among the flat-plate results in that a frequency-selective amplification is clearly evident. The case 2.2 is considered first because certain stability theory results are available and because a wider range in R was covered in the experiments. The curve for the most forward station, $R = 415$, shows that the boundary layer is more receptive to low-frequency disturbances than to high ones in the region ahead of the measurement station. In the subsequent development of A/A_∞, it can be seen that frequency-dependent growth occurs such as to produce a broad peak which shifts to ever-lower frequency with increasing R. In addition, high frequency damping occurs for $R \gtrsim 1000$. The energy profile through the boundary layer for the last station, $R = 1360$, was strongly nonsimilar. There, turbulent bursts were seen in the signal, and these account for the extremely rapid growth of the high-frequency waves observed.

Three theoretical response curves A/A_o for 60° waves are included in the figure. Because the relation between A_o, the neutral-point amplitude, and A_∞ is unknown, the curves have been jointly adjusted in magnitude by an arbitrary factor such as to bring the $R = 1000$ curve to the approximate level of the $R = 1010$ data. The spectrum of wave angles is also unknown. However, the 60° results represent a limiting case because the waves grow most rapidly for this angle. The predicted and measured responses at $R = 1000$ and 1010 are seen to be similar over most of the frequency range. The $R = 800$ and 1200 curves indicate a theoretical growth rate less than that observed (Sec. III-C), and predict a narrowing of the response which is not in accordance with the data.

The available A/A_∞ data for $M_\infty = 1.6$ resemble those at 2.2 in that frequency-selective amplification and damping again take place, but differ in regard to the general level at a corresponding value of R. A portion of the theoretical response curve for $R = 1000$, $\psi = 60°$ has been computed, but is not shown here. The peak occurs at $F = 0.33 \times 10^4$, in agreement with the frequency interpolated from the data.

It is evident at this M_∞, as well as at 2.2, that the layer is receptive to low frequency disturbances in the vicinity of the plate leading edge. Several measurements were carried out at $M_\infty = 1.6$ in which profiles of the energy for various frequencies $0.14 < F \times 10^4 < 0.50$ were recorded at several stations ahead of $R = 600$. The measurements showed that the fluctuations were either constant or declining slightly with R, with amplitudes corresponding to those shown in Fig. 3a. Thus, freestream disturbances seem to enter the layer at the leading edge, as has already been proposed by Laufer and Vrebalovich.[13]

The situation at $M_\infty = 3.0$, 4.5, and 5.6 differs from that at lower speeds. Figs. 3c–3f show that the amplitudes of waves of all frequencies grow monotonically larger with increasing R, except for $M_\infty = 4.5$, $R = 1345$, and 1470, which are in the nonlinear region. The growth is less frequency-selective than at the lower speeds.

Discussion is limited to the case $M_\infty = 4.5$. The available portion of the predicted first-mode response curve A/A_o for $R = 1000$, $\psi = 60°$, adjusted in level to conform to the data as described previously for $M_\infty = 2.2$, is included in Fig. 3e. The curve is intended to show that the shapes of the observed and predicted responses are generally similar in the overlapping frequency range. In addition, the curve indicates that the first mode extends to higher frequencies than those to which the experiments are limited by the rapid rolloff of the energy spectrum. The second mode lies at even higher frequencies. Mack shows in Fig. 12.24 of Ref. 10 that the most-amplified second mode disturbances for $R = 1500$ occur at about $F = 1.4 \times 10^{-4}$. Extrapolation of the measured freestream spectra to this frequency indicate that the fluctuations there are probably more than 40 db below those at the low end of the frequency spectrum. Thus, the second mode may not play an important role in the transition process in comparison to the nonlinearity of the low-frequency waves.

The results for $M_\infty = 3.0$ and 5.6 are sufficiently similar to those of 4.5 that the fluctuation development for all three speeds is probably much the same. The results for $M_\infty = 8.5$ are described separately in Sec. III-F.

C. Comparison with Theory, $M_\infty = 2.2$ and 4.5

The A/A_∞ curves for $M_\infty = 2.2$ (Fig. 3b) together with further data of a similar type for $Re = 3.4$ and 5.0×10^4 cm^{-1} were used to determine the amplification rate α_i at $R = 1000$ for comparison with the theory. This station is sufficiently far ahead of that at which the energy profiles show a departure from similarity that nonlinear effects do not seem to be a problem. The logarithmic differentiation involved in the determination of α_i minimizes the uncertainties in the level of the A/A_∞ data, but the fairly large increments in R preclude high accuracy.

The results, shown in Fig. 4, indicate that the frequency of the peak growth rate is accurately predicted, but that the range of unstable frequencies and the rates of growth are not in agreement. Somewhat similar results were obtained in the Laufer-Vrebalovich stability experiment.[13] The reason for the disagreement between theory and experiment is not known.

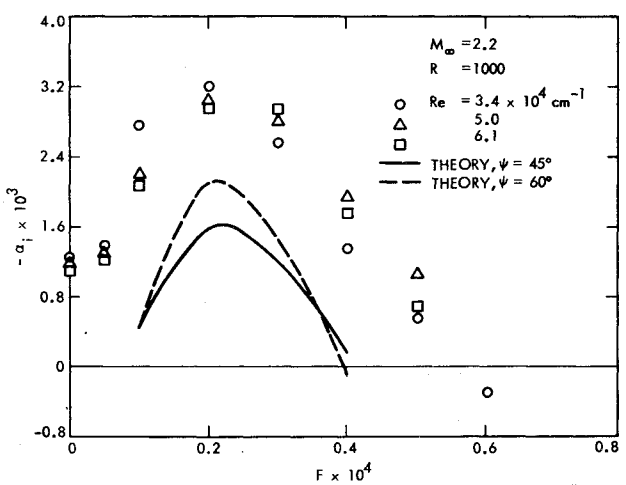

Fig. 4 Comparison with stability theory, $M_\infty = 2.2$.

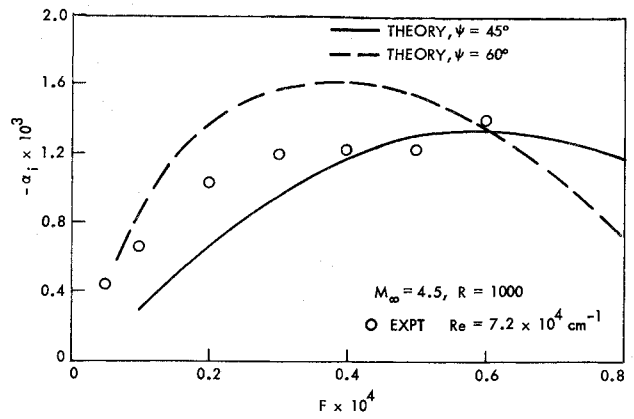

Fig. 5 Comparison with stability theory, $M_\infty = 4.5$.

The $M_\infty = 4.5$ data of Fig. 3e have been converted to amplification rate form and are shown in Fig. 5. Unfortunately, the results do not extend to sufficiently high frequencies to cover all the first mode range. However, such results as are available are in much better agreement with the theory than at $M_\infty = 2.2$. As mentioned earlier, the theory has been verified at $M_\infty = 4.5$.[8]

A simultaneous test of the stability and forcing theories for $M_\infty = 4.5$ is presented in Fig. 6. There, some of the data of Figs. 3d and e are compared with theoretical results for three frequencies which span most of the measurable spectrum. The measured reference amplitudes A_{∞} have been divided by two, corresponding to a doubling of A/A_{∞}, in order to improve the agreement with theory. However, there is a reason why an adjustment is appropriate. A_{∞} was measured by placing the hot-wire ahead of the test plate, where it was exposed to waves arriving from all directions. It is expected that waves arriving from the lower half of the tunnel do not affect the plate topside boundary layer, and thus the measured A_{∞} is too large. Assuming that the top and bottom-half waves were uncorrelated, each should have contributed equal signal power, so that the measured A_{∞} was larger by $(2)^{1/2}$ than if only the top half waves had been present. The factor 2 has been used in preference to $(2)^{1/2}$ in order to emphasize the similarity of the observed and predicted growths.

The theoretical curves are a composite of the forcing theory and the stability theory. For each frequency, the forcing theory results for $\psi = 0°$, $c_p = 0.65$, have been used for all values of R up to that at which the peak response occurs. This point is not greatly different than the neutral point, for which $A/A_o = 1$ in the stability theory. All subsequent amplification is presumed to take place according to the stability results for $\psi = 60°$, with the initial amplitude being matched to the forcing result.

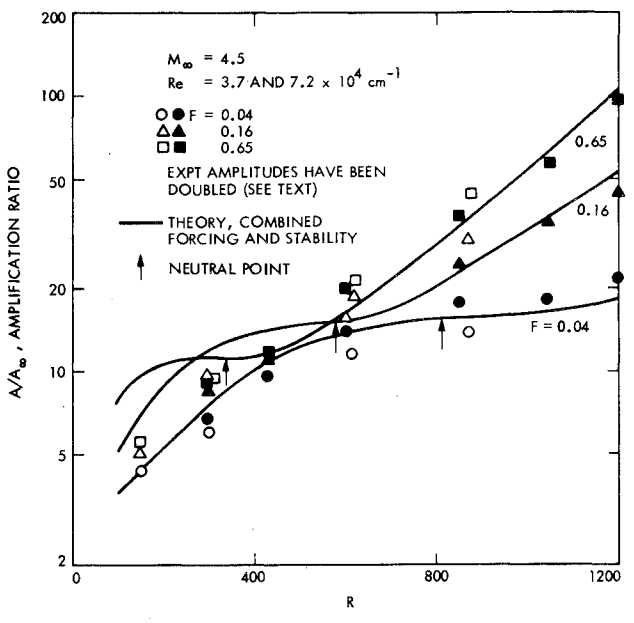

Fig. 6 Comparison with combined theory, $M_\infty = 4.5$.

The mismatch of assumed wave angles at the point of juncture presents a question which cannot be settled now because the spectrum of angles is unknown. It will be conjectured in Sec. 3E that the waves are mostly oblique, as is appropriate to the stability theory. The effect of ψ on the forcing theory has not been thoroughly investigated but the available results[11] indicate that the forcing theory is less sensitive to angle than is the stability theory.

Figure 6 shows that for each frequency the experimental amplitudes of the two Re cases are in reasonable agreement with each other, and that the levels and trends of the theoretical curves bear considerable resemblance to the data. Similar agreement prevails at the intermediate frequencies $F = 0.08$ and 0.32, omitted here. It is to be noted that for the higher Re case, transition was observed at $R \simeq 1500$; $R = 1200$ is close to the start of nonlinearity as determined from a clearly-evident flattening of the hot-wire signal described in Sec. III-G.

D. Correlation Measurements

An indication of the relative coupling between the freestream disturbances and those in the boundary layer can be obtained by cross-correlating the signals of a probe placed in the stream and of one in the layer. For this purpose, a probe was affixed to the underside of the test plate such that the hot wire was 0.1 cm or less directly below the sharp leading edge, slightly ahead of the shock formed by the bevel. The wake of the probe was swept below the plate. The signal of a second probe in the topside layer was correlated with that of the first. The results for several Mach numbers are shown in Fig. 7 for the case of the second probe at $x = 5.0$ cm, y at the location of the energy peak and with the probes being in lateral alignment. The data for $M_\infty = 3.0$ pertain to the outer of the two energy peaks, which occur at $y/\delta \simeq 0.49$ and 0.74 for all values of the wire overheat. The correlation pattern at the inner peak resembles that shown here except for an expansion of the time delay by about 5%.

The figure indicates that a wave incident upon the plate leading edge results in a boundary-layer disturbance which arrives at the downstream wire at a later time. Measurements of the wave propagation and dispersion at $M_\infty = 4.5$ have been discussed in an earlier report.[19] The results shown here indicate that the degree of correlation rises monotonically with M_∞. This result has an important consequence. For the higher Mach numbers, the boundary-layer fluctuations are almost certainly caused by

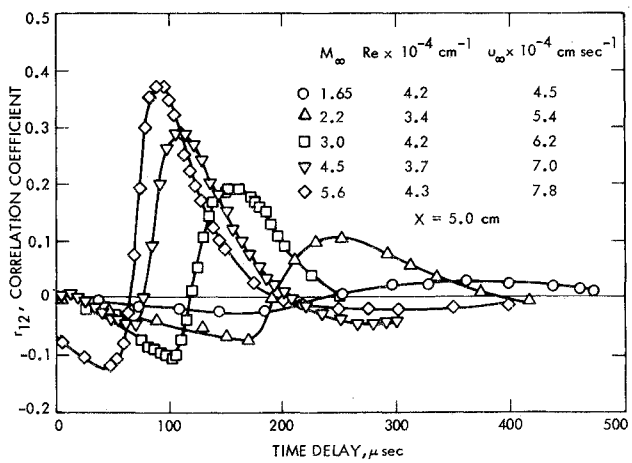

Fig. 7 Cross-correlation of freestream and boundary-layer fluctuations.

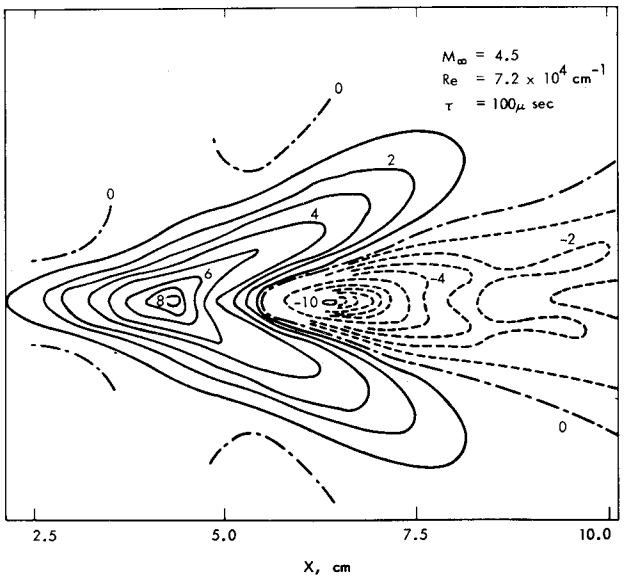

Fig. 8 Iso-correlation contours in boundary layer.

the freestream sound; for the lower speeds, the fluctuations are perhaps not the result of the sound waves, but rather of some other source of unsteadiness masked by the sound. Further investigation on this matter is needed.

E. Wave Obliquiness

The lack of wave obliqueness information has been seen to make difficult the interpretation of several results. An attempt to gain such information was carried out at $M_\infty = 4.5$ by use of the correlation technique. The experimental setup was precisely that described earlier: the signal of a probe in the boundary layer at the energy peak was correlated with the delayed signal of a probe at the plate leading edge. Here, the lateral and streamwise positions of the downstream probe were varied. Figure 8 shows the iso-correlation contours for a time delay of 100 μsec. The values of the correlation are arbitrary. The probes were in lateral alignment at the approximate symmetry line of the pattern. The Fourier transform of the pattern, yet to be computed, will be needed to determine the obliqueness spectrum. However, an indication of wave obliquity can be inferred from the orientation of the lobes. Similar measurements at 200 and 300 μsec time delay show that the pattern grows larger and less distinct with increase of time, perhaps as a result of wave dispersion.

F. Hypersonic Results

It has been reported in a number of experiments that large amplitude, laminar, periodic waves appear and persist ahead of transition in hypersonic cone boundary layers.[5,17,20,21] A photograph included here as Fig. 9a was obtained by Demetriades,[17] no photographs having been taken in the present hypersonic tests.

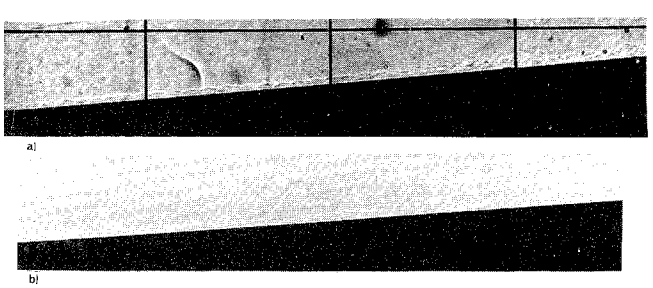

Fig. 9 Transition zone shadowgraphs: a) 5° Cone, $M_\infty = 8.0$ (Courtesy A. Demetriades); b) 4° Cone, $M_\infty = 4.5$.

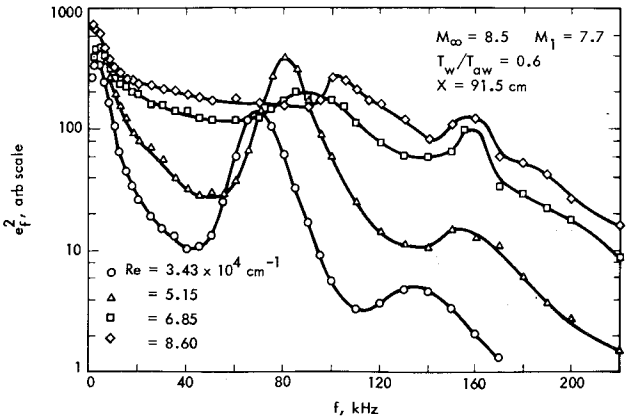

Fig. 10 Boundary-layer fluctuation spectra, $M_\infty = 8.5$.

Evidence of such waves, and of smaller amplitude ones preceding them, has been obtained here. The hot-wire signals showed at least some periodicity at all locations in the boundary layer over the range of Reynolds numbers tested. The periodicity was most evident at the y location of the fluctuation peak for the downstream positions and at the higher Reynolds numbers.

Figure 10 presents the fluctuation spectra measured at a particular cone station for four values of the unit Reynolds number. For the two lower Re cases, the periodicity of the flow at about 70–80 kHz is quite evident. These are the principal oscillations, and will later be identified with second mode instability. The wavelength of these can be equated to that appearing in the photograph of Fig. 9a as follows. For waves moving with the stream velocity, 1.1×10^5 cm sec^{-1}, the length of the 70 kHz waves would be 1.5 cm. The wavelength to computed boundary-layer thickness ratio is then about 2.2, a value consistent with that seen in the photograph.

In addition to the 70–80 kHz oscillations, there are spectral features at about 140–160 kHz which are quite possibly the result of third-mode instability. Demetriades[17] has reported finding periodicities corresponding to these, as well as the much stronger second-mode oscillations.

The results for the two higher values of Re serve to confuse rather than clarify the succession of events. It is seen that the periodicity is substantially reduced and that there is a general rise in the high frequency energy. This combination of circumstances might be taken as an indication that transition to turbulence was in progress. However, such was probably not the case. A few minutes later during the same run, waveform photographs were taken, and it was clearly evident from the strong periodicity that the flow was not transitional. Other photographs at the highest Re, 10.7×10^4 cm^{-1}, were equally "clean." In retrospect, the most probable cause of the loss of periodicity at the higher Reynolds numbers was a failure to maintain the hot wire at the optimum y-location as the tunnel pressure was increased.

Figure 11 compares two fluctuation spectra measured inside the boundary layer at the energy peak and outside the layer at $y/\delta \simeq 4$ for the lowest unit Reynolds number case. These spectra were used to prepare the results shown in Fig. 3g. It can be seen here and in Fig. 3g that the boundary-layer fluctuations mirror those of the stream for frequencies below 30–40 kHz, being larger by a relatively constant factor. At about 40–50 kHz, there is a definite departure in shape due to the boundary-layer instability.

All amplification rate experiments were carried out at the lowest value of Re in order to avoid the nonlinear wave region. Figure 12 presents the amplification rate data determined from the slopes of the $e_f^2(x)$ curves. Each curve is faired through the data pertaining to a particular x station. The figure shows that the amplification is low at low frequencies, rises with frequency to a definite peak, subsides to a damped frequency

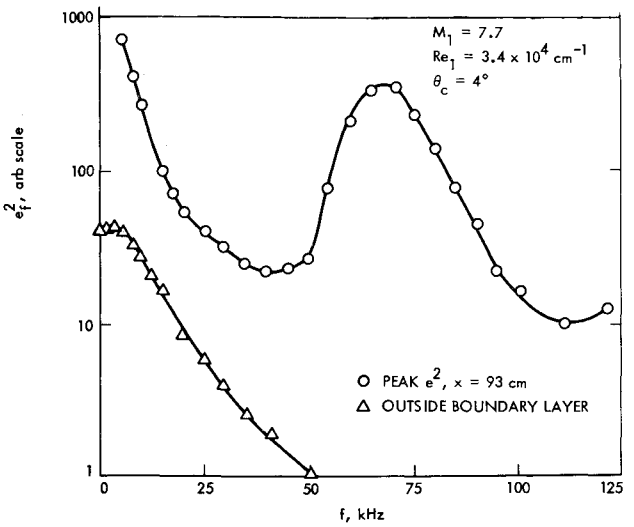

Fig. 11 Fluctuation spectra in boundary layer and in stream, $M_\infty = 8.5$.

range, and finally exhibits a second amplified region. Unfortunately, a declining signal-to-noise ratio prevented continuation of the measurements to higher frequencies, and some of the scatter at the highest frequencies may have resulted from noise problems.

The amplified frequency regions seen here can be identified with the spectral features of the corresponding Reynolds number curve of Fig. 10. The 70 kHz peak of Fig. 10 has a corresponding value of $F = 1.17 \times 10^{-4}$, and thus lies near the lower most-unstable frequency. The less prominent feature at 135 kHz, for which $F = 2.25 \times 10^{-4}$, lies near the cutoff frequency. The smaller proportions of the 135 kHz peak imply that the extent of the upper unstable region does not exceed that of the lower region. It has already been speculated that the upper region may correspond to third mode instability.

Figure 13 presents a comparison between some of Mack's recent unpublished amplification rate computations and those experimental data of Fig. 12 for the station $R = 1740$ which lie in the corresponding frequency range. The theoretical results, which pertain to the two-dimensional case, have been adjusted to apply to the cone-flow case. The cone boundary layer is thinner than the plate layer by a factor of $(3)^{1/2}$. In order that the amplification rate $(\delta/e^2)(de^2/dx)$ be preserved, the dimensionless rate of the theory has been increased by $(3)^{1/2}$ for inclusion in Fig. 13. In addition, the value of $R = 1000$, at which the theory is applied, is approximately equal to the value of R

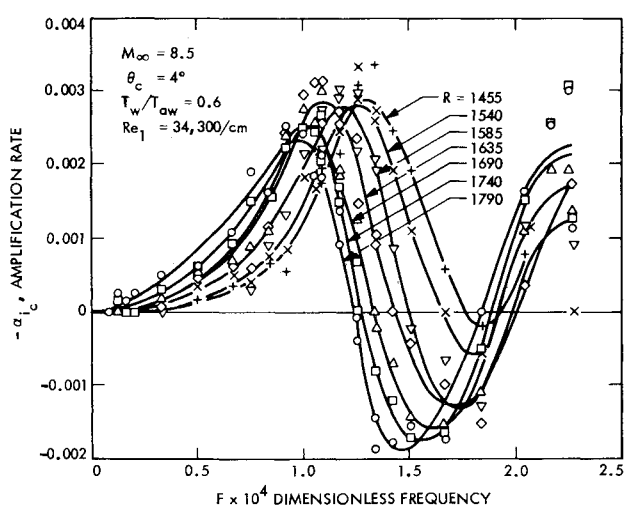

Fig. 12 Spatial amplification rate, $M_\infty = 8.5$.

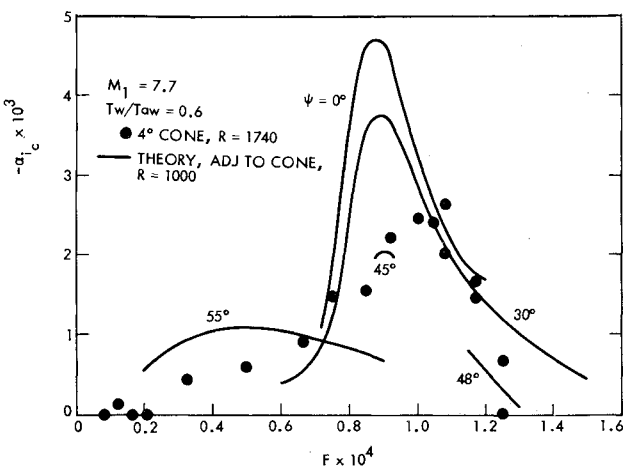

Fig. 13 Comparison with stability theory, $M_\infty = 8.5$.

on the cone reduced by $(3)^{1/2}$ in order that the boundary-layer thickness Reynolds numbers be of equal magnitude. The relation between cone and flat plate stability is discussed in the Appendix of Mack's paper.[12]

The several curves of the figure represent first and second mode theoretical results for various values of the wave obliqueness angle, ψ. The lowest frequency curve pertains to first mode oscillations, whereas all other curves are for second mode oscillations. For the present flow conditions, the first-mode waves are most amplified when $\psi = 55°$, and so the curve shown represents the highest growth rate to be expected. As indicated earlier, second-mode waves are most amplified for $\psi = 0°$.

As before, no direct information on the wave obliqueness is available to aid in selecting the correct theoretical result for comparison with experiment. However, it is probable that the wave structure seen in the photograph is approximately two-dimensional, since periodic waves with substantial obliqueness would not have been recorded.

The theoretical curves show that the frequency of the most-unstable second-mode waves is nearly independent of ψ, and that this frequency is about 15% below that of the experimentally-observed most-unstable waves. The peak of the predicted amplification rate for $\psi = 0°$, i.e., the angle believed to be most appropriate, is nearly twice that measured. Although the agreement in amplification rate is not very good, the reasonably good agreement in frequency serves to identify the periodic waves as being of the second-mode type with considerable certainty.

A somewhat similar comparison between theory and experiment prevails in the first-mode frequency range. The theoretical amplification rates again exceed the measured values. However, the general concurrence that the amplification rates are low in comparison to the second-mode rates for the present wall-cooling ratio is regarded as significant because of the strong effect of cooling on first-mode instability.

G. Breakdown to Turbulence

Certain qualitative observations on the breakdown of the laminar fluctuations to turbulence are described here. For $M_\infty = 2.2$, at least two stages of development could be seen. In the first, the energy profiles through the layer for $R \gtrsim 1200$–1300 showed an increasingly rapid departure from similarity as mentioned earlier, with the profiles developing high frequency energy in a concentrated layer of thickness 0.07–0.10δ, and located at about $y/\delta = 0.6$. The energy rises abruptly with frequency for values of $F \times 10^4 \gtrsim 0.6$. The hot-wire signal within this layer indicates that the fluctuations have a very definite limit of excursion. Each cycle is rather indefinite in wavelength, but the peak value in either direction is similar from wave to wave.

In the second stage, turbulent bursts which reasonably could be attributed to the passage of turbulent spots were evident in the hot-wire signal. The distinguishing characteristic of a burst

is a rapid rise in the fluctuation intensity, with the signal containing much energy at frequencies corresponding to wavelengths less than the boundary-layer thickness. Spangenberg and Rowland[22] have used optical methods to carry out a detailed study of the spot production frequency, growth rate, and propagation speeds at a similar Mach number, 1.96.

At $M_\infty = 4.5$ and 5.0, a different sequence of events was found for the case of an adiabatic wall than for a cooled wall. For the former, the laminar fluctuations described in Secs. III-B and III-C became amplitude-limited, i.e., showed definite limits of excursion, in the region $R \gtrsim 1200$. With further increase of R, the hot-wire signal showed an ever-increasing complexity of waveform and an evolution into a turbulent state without definite evidence of turbulent bursts. A shadowgraph illustrating this is given in Fig. 9b. Of 10 such photographs showing both the top and bottom surfaces of the cone, only one showed a different progression. There, a short, almost-turbulent disturbance appeared at both the top and bottom of the cone, about 25δ ahead of the usual transition zone. Fischer[23] has reported finding turbulent "rings" on a cone at a hypersonic speed. The one incident reported here seems to show that a similar behavior is possible, if not probable, at this lower speed.

For the case of the 96-cm cooled 4° cone in the 21-in. hypersonic tunnel at $M_\infty = 5.0$, $M_1 = 4.8$, $Re_1 = 8.7 \times 10^4$ cm^{-1}, the boundary layer showed no bursts ahead of the transition at $Re_x = 6.0 \times 10^6$ for a wall temperature $T_w = 0.6T_{aw}$. Upon lowering the temperature below this level, bursts became clearly evident, and ceased abruptly as the wall warmed again.

IV. Conclusions

Microscopic experiments relating to fluctuation sources and amplification mechanisms give the following indications. The wind tunnel sound is of sufficient intensity to present a potentially important source of boundary-layer disturbances for all values of M_∞ tested here. However, it was found that the correlation coefficient between freestream and boundary-layer fluctuations was rather low at $M_\infty = 1.6$ and 2.2, raising a question as to whether the sound might be less effective than some other unsteadiness in disturbing the layer at these speeds. Velocity and temperature fluctuations which are immeasurably small in the test section in comparison with the sound, cannot be excluded as possible sources. Whatever the origin, the fluctuations appear in the layer ahead of the forwardmost station of measurement for these two Mach numbers.

It becomes increasingly certain as the Mach number rises from 3.0 to 5.6 that the sound field drives the boundary layer. Not only does the degree of correlation between the stream fluctuations and those in the layer increase with M_∞, but the boundary-layer response at low values of R then shows a behavior consistent with expectations based on forcing theory. At $M_\infty = 4.5$, a direct comparison of observation with forcing theory was reasonably good for a wide range of frequencies up to the station $R \simeq 500$. At $M_\infty = 8.5$, the evidence is less direct, and rests on the relative constancy of the ratio of boundary layer to freestream fluctuation amplitudes across the frequency spectrum up to, but not including, the second mode range.

The amplification rates determined here are expected to be relevant to a wider variety of flows than are the disturbance-source results, which pertain to a particular facility. The evidence for instability amplification was obtained through a comparison of the frequency and of the growth rate observed with that predicted by the linear theory. The comparison showed that the theory predicted the most-amplified frequency to within 10 or 15 percent over the full Mach number range. However, the growth rate was not given so well in all cases.

At $M_\infty = 2.2$, the amplification rate for all stations well ahead of that at which nonlinearity produced a departure from similarity was considerably higher than that predicted. For $R = 1000$ in particular, the peak growth rate was approximately twice that predicted for even the most unstable wave angle, $\psi = 60°$, and the unstable frequency range was about twice as wide as expected. At $M_\infty = 4.5$, however, reasonably good agreement prevailed over the measurable frequency range. It should be noted that the freestream rms mass-flow fluctuation at this Mach number is of the order of one percent, and that the boundary layer increases this level about tenfold by means of the forcing mechanism ahead of the neutral point. Moreover, the peak-to-peak fluctuation exceeds the rms level by several times. In view of this high disturbance level, it is perhaps surprising that the subsequent amplification is linear.

The hypersonic results show a remarkable difference with respect to those at lower speeds. Somewhere between Mach number 5.6 and 7.7 ($M_\infty = 8.5$), the second mode appears as the dominant instability, and is able by means of a long run of amplification to single out a narrow band of high frequencies from the intense stream disturbances. The effect is to produce the well-ordered "rope-like" waves seen in photographs, which persist for relatively long distances, and which culminate in transition.

Although the theory predicts that second mode waves are very unstable at $M_\infty = 4.5$, and especially at 5.6, none is visible in photographs of the transition zone such as that shown in Fig. 9b. The question of why the dominant instability switches modes in the brief Mach range between 4.5 and 7.7 is probably connected with the frequency. Reshotko[18] has pointed out that the second-mode frequency in a supersonic wind tunnel is very high. Mack shows in Fig. 12.24 of Ref. 10 that the frequency of the second mode at $M_\infty = 4.5$, $R = 1500$ is nearly twice as high as at $M_\infty = 7.7$. There is then less energy available for amplification on account of the rolloff of the frequency spectrum. Moreover, the cooling required with air as the hypersonic test medium has cut the first mode amplification rate and slightly enhanced the second mode, according to theory.

References

[1] Morkovin, M. V., "Critical Evaluation of Transition from Laminar to Turbulent Shear Layers with Emphasis on Hypersonically Traveling Bodies," AFFDL-TR-68-149, March 1969, Air Force Flight Dynamics Lab., Wright-Patterson Air Force Base, Ohio.

[2] Laufer, J., "Stability of the Laminar Boundary Layer," *Symposium on Boundary Layer Research*, Freiburg, International Union of Theoretical and Applied Mechanics, Springer-Verlag, Berlin, 1958, pp. 139–140.

[3] Laufer, J., "Aerodynamic Noise in Supersonic Wind Tunnels," *Journal of the Aerospace Sciences*, Vol. 28, No. 9, Sept. 1961, pp. 685–692.

[4] Laufer, J., "Some Statistical Properties of the Pressure Field Radiated by a Turbulent Boundary Layer," *Physics of Fluids*, Vol. 7, No. 8, Aug. 1964, pp. 1191–1197.

[5] Stainback, P. C., Fischer, M. C., and Wagner, R. D., "Effects of Wind-Tunnel Disturbances on Hypersonic Boundary Layer Transition," AIAA Paper 72-181, San Diego, Calif., 1972.

[6] Donaldson, J. C. and Wallace, J. P., "Flow Fluctuation Measurements at Mach 4 in the Test Section of the 12-Inch Supersonic Wind Tunnel (D)," AEDC-TR-71-143, Aug. 1971, Arnold Engineering Development Center, Arnold Air Force Station, Tenn.

[7] Pate, S. R. and Scheuler, C. J., "Radiated Aerodynamic Noise Effects on Boundary-Layer Transition in Supersonic and Hypersonic Wind Tunnels," *AIAA Journal*, Vol. 7, No. 3, March 1969, pp. 450–457.

[8] Kendall, J. M., "Supersonic Boundary Layer Stability Experiments," *Proceedings of Boundary Layer Transition Study Group Meeting*, Vol. II, Aerospace Corp., San Bernardino, Calif., Aug. 1967.

[9] Laufer, J., "Factors Affecting Transition Reynolds Numbers on Models in Supersonic Wind Tunnels," *Journal of Aeronautical Sciences*, Vol. 21, No. 7, July 1954, pp. 497–498.

[10] Mack, L. M., "Boundary Layer Stability Theory," Rept. 900-277 Rev. A, Nov. 1969, Jet Propulsion Lab., Pasadena, Calif.

[11] Mack, L. M., "Progress in Compressible Boundary Layer Stability Computations," *Proceedings of the Boundary Layer Transition Workshop*, Vol. IV, Aerospace Corp., San Bernardino, Calif., Dec. 1971.

[12] Mack, L. M., "On the Application of Linear Stability Theory to the Problem of Supersonic Boundary Layer Transition," *AIAA Journal* (this issue).

[13] Laufer, J. and Vrebalovich, T., "Stability and Transition of a Supersonic Laminar Boundary Layer on an Insulated Flat Plate," *Journal of Fluid Mechanics*, Vol. 9, Part 2, Oct. 1960, pp. 257–299.

[14] Demetriades, A., "An Experiment on the Stability of Hypersonic Boundary Layers," *Journal of Fluid Mechanics*, Vol. 7, Pt. 3, March 1960, pp. 385–396.

[15] Potter, J. L. and Whitfield, J. D., "Effects of Slight Nose Bluntness and Roughness on Boundary Layer Transition in Supersonic Flows," *Journal of Fluid Mechanics*, Vol. 12, Pt. 4, April 1962, pp. 501–535.

[16] Staylor, W. F. and Morrisette, E. L., "Use of Moderate Length Hot-Wires to Survey a Hypersonic Boundary Layer," *AIAA Journal*, Vol. 5, No. 9, Sept. 1967, pp. 1698–1700.

[17] Demetriades, A., "Hypersonic Viscous Flow over a Slender Cone; Part III: Laminar Instability and Transition," AIAA Paper 74-535, Palo Alto, Calif., 1974.

[18] Reshotko, E., "Stability Theory as a Guide to the Evaluation of Transition Data," *AIAA Journal*, Vol. 7, No. 6, June 1969, pp. 1086–1091.

[19] Kendall, J. M., "JPL Experimental Investigations," *Proceedings of the Boundary Layer Transition Workshop*, Vol. IV, Aerospace Corp., San Bernardino, Calif., Dec. 1971.

[20] Potter, J. L. and Whitfield, J. D., "Boundary-Layer Transition under Hypersonic Conditions," AGARDograph 97, Pt. III, May 1965, pp. 1–61.

[21] Fischer, M. C. and Weinstein, L. M., "Cone Transitional Boundary-Layer Structure," *AIAA Journal*, Vol. 10, No. 4, April 1972, pp. 699–701.

[22] Spangenberg, W. G. and Rowland, W. R., "Optical Studies of Boundary Layer Transition Processes in a Supersonic Air Stream," *Physics of Fluids*, Vol. 3, No. 5, Sept.–Oct. 1960, pp. 667–684.

[23] Fischer, M. C., "Turbulent Bursts and Rings on a Cone in Helium at $M_e = 7.6$," *AIAA Journal*, Vol. 10, No. 10, Oct. 1972, pp. 1387–1389.